Nanoscale

PAPER

View Article Online
View Journal | View Issue

Cite this: *Nanoscale*, 2016, **8**, 590

Intracellular degradation of chemically functionalized carbon nanotubes using a long-term primary microglial culture model†

Cyrill Bussy,[a,b] Caroline Hadad,[c,d] Maurizio Prato,[c,d] Alberto Bianco[e] and Kostas Kostarelos*[a,b]

Chemically functionalized carbon nanotubes (f-CNTs) have been used in proof-of-concept studies to alleviate debilitating neurological conditions. Previous *in vivo* observations in brain tissue have suggested that microglia – acting as resident macrophages of the brain – play a critical role in the internalization of f-CNTs and their partial *in situ* biodegradation following a stereotactic administration in the cortex. At the same time, several reports have indicated that immune cells such as neutrophils, eosinophils and even macrophages could participate in the processing of carbon nanomaterials *via* oxidation processes leading to degradation, with surface properties acting as modulators of CNT biodegradability. In this study we questioned whether degradability of f-CNTs within microglia could be modulated depending on the type of surface functionalization used. We investigated the kinetics of degradation of multi-walled carbon nanotubes (MWNTs) functionalized *via* different chemical strategies that were internalized within isolated primary microglia over three months. A cellular model of rat primary microglia that can be maintained in cell culture for a long period of time was first developed. The Raman structural signature of the internalized f-CNTs was then studied directly in cells over a period of up to three months, following a single exposure to a non-cytotoxic concentration of three different f-CNTs (carboxylated, aminated and both carboxylated and aminated). Structural modifications suggesting partial but continuous degradation were observed for all nanotubes irrespective of their surface functionalization. Carboxylation was shown to promote more pronounced structural changes inside microglia over the first two weeks of the study.

Received 24th September 2015,
Accepted 25th November 2015

DOI: 10.1039/c5nr06625e

www.rsc.org/nanoscale

Introduction

Surface functionalization of CNTs able to alter the hydrophobic character of pristine materials and therefore allow their use under physiological conditions has been shown to also greatly enhance their overall biocompatibility compared to unmodified CNTs.[1] Chemically functionalized carbon nanotubes (f-CNTs) have been proposed for a broad range of biomedical applications,[2] including neurology. CNTs have been studied for their suitability as substrates for neurite outgrowth, as components in implants or electrodes, and as drug or gene delivery systems for brain disorders.[3]

Amine-functionalized single-walled CNTs, directly injected in mouse brain ventricles, were shown to reduce the impact of ischemia and inflammation and offer neuroprotective effects.[4] We have previously demonstrated that MWNTs covalently functionalized by 1,3-dipolar cycloaddition reaction were able to carry Caspase 3 siRNA into neurons, in order to alleviate ischemia-induced damage in the motor cortex of animals.[5] In these studies, f-CNTs were directly administered into the brain (ventricles or parenchyma). It is crucial to better understand the interactions of f-CNTs with the resident brain cells and their fate after injection. In addition, determination of the physicochemical nanotube features (such as length or surface character) as determinants of these interactions are largely ignored. Recently, we have shown *in vivo* that MWNTs that were oxidized prior to being amino-functionalized were able to induce a sustained inflammatory response and glial cell activation in areas peripheral to the injection site,

[a]*Nanomedicine Lab, School of Medicine & National Graphene Institute, University of Manchester, AV Hill Building, Manchester M13 9PT, UK. E-mail: kostas.kostarelos@manchester.ac.uk*
[b]*Faculty of Life Sciences, University College London, Brunswick Square, London WC1N 1AX, UK*
[c]*Center of Excellence for Nanostructured Materials, Department of Chemical and Pharmaceutical Sciences, University of Trieste, Trieste, Italy*
[d]*Carbon Nanobiotechnology Laboratory, CIC biomaGUNE, Paseo de Miramón 182, 20009 Donostia-San Sebastian, Spain*
[e]*CNRS, Institut de Biologie Moléculaire et Cellulaire, UPR 3572, Immunopathologie et Chimie Thérapeutique, Strasbourg, France*
†Electronic supplementary information (ESI) available. See DOI: 10.1039/c5nr06625e

whereas amino-functionalized MWNTs were only eliciting local and transient responses under similar conditions.[6] This suggested that the type of surface functionalization is an important component of the cellular responses of the brain tissue to f-CNT exposure.

CNTs have been thought to be non-degradable materials under physiological conditions due to a strong and chemically inert sp^2 graphitic structure. However, in the last few years, several *in vitro* and *in vivo* reports have shown that CNTs can undergo an oxidation-mediated biodegradation under specific conditions present in responsive immune cells.[7] These findings indicated that biodegradation of carbon nanomaterials may require inflammation and the generation of reactive oxygen species to take place.[8,9] In addition, carbon nanomaterials bearing oxygenated groups (*i.e.* hydroxyl, carbonyl, carboxyl functions) were proven to be more degradable than carbon nanomaterials that have no or limited amount of oxygenated functions on their surface showing again the importance of surface chemistry.[10–12] Based on those studies, the concept of degradation-by-design was experimentally confirmed.[13] In this study, carbon nanotube surface was chemically modified to enhance the enzyme mediated degradation of the nanotubes. With regards to central nervous system (CNS), we have recently demonstrated that amino-functionalized MWNTs were undergoing structural deformations leading to partial degradation even two days after stereotactic injection into the mouse brain cortex, and that this degradation process was taking place in microglia.[14] An alteration of the graphitic structure of oxidized MWNTs suggesting intracellular processing was also observed after a short period of time (24–72 h) in immortalized N9 microglial cells.[15] Nevertheless, knowledge on f-CNT degradation following cellular internalization within microglial cells remains limited and requires further investigations in particular to reveal the degradation kinetics and the physicochemical determinants of f-CNT degradability in the brain. Taken into account the important role of surface properties in terms of cell responses and biodegradability of carbon nanomaterials, we hypothesized that microglia-mediated degradation of f-CNTs will vary with the type of surface functionalization.

In this study, three different types of covalently functionalized f-MWNTs were used and the structural evolution of the internalized materials within primary microglial cells isolated from rat embryonic brain was directly assessed *via* Raman spectroscopy, a sample preparation – free technique, at different time points over 3 months. The aim of this study was to investigate *in situ* whether the type of surface functionalization influenced the degradability of f-MWNTs, and to describe the kinetics of degradation in a primary cellular model in the long-term using long-lasting non-dividing cells. We report that isolated primary microglia have the ability to internalize, contain and continuously degrade over time various f-CNTs irrespective of their surface functionalization, although carboxylation allowed faster structural deformation in the first two weeks of the study. Notably, f-MWNTs were still present in the primary microglial cells even 3 months after their initial internalization, suggesting that microglia can store f-CNTs for a long period of time without apparent damages, and that degradation in isolated microglia can occur in a slow but continuous process.

Results and discussion

Chemical structure and characterisation of MWNT suspension

Three different chemically functionalized MWNTs were synthesized from the same batch of pristine starting material to eliminate variations in the content of metal (or other) impurities. Fig. 1a shows the chemical structure of the f-MWNTs studied that included: (i) carboxylated MWNTs (ox-MWNTs) prepared by treatment in strong acid conditions;[16] (ii) amino-functionalized oxidised MWNTs (ox-MWNT-NH_3^+) prepared by 1,3 dipolar-cycloaddition reaction after their initial oxidation as previously described, hence both ox-MWNTs and ox-MWNT-NH_3^+ have the same amount of carboxylic functions;[14] and (iii) amino-functionalized MWNTs (MWNT-NH_3^+) prepared following the 1,3 dipolar-cycloaddition reaction on pristine MWNTs as previously reported.[17,18] Functionalized MWNTs that have undergone oxidation are shorter (200–300 nm in length for ox-MWNT and ox-MWNT-NH_3^+) than the f-MWNTs without initial oxidation (*i.e.* MWNT-NH_3^+) which kept a similar length as the pristine starting material (between 0.5–2 μm).

The degree of amino group loading on the side walls and tips of the f-MWNTs as determined by the Kaiser test is summarized in Fig. 1b. All MWNT suspensions were prepared in 5% dextrose using bath sonication and they exhibited good aqueous dispersibility prior to their incubation within cells. The Raman spectroscopy analysis of the different f-MWNT suspensions revealed the characteristic peak at 1330 cm^{-1} (D band), 1585 cm^{-1} (G band) and 1620 cm^{-1} (D′ band) for all nanotubes (Fig. 1c). Oxidation of nanotubes that introduced carboxyl groups in their graphitic lattice as well as shortening, also led to higher amount of structural defects as reflected by a more pronounced and intense D′ band for both ox-MWNT and ox-MWNT-NH_3^+ compared to MWNT-NH_3^+ that was functionalized without prior oxidation (Fig. 1c). For MWNT-NH_3^+, the D′ band only appeared as a shoulder on the G band of the Raman spectra, suggesting a less defected structure compared to the other two materials. These results are in agreement with a previous report showing that oxidation could induce an increase of defects that can be assessed *via* Raman spectroscopy.[19]

Live imaging of primary microglia cell culture exposed to functionalized carbon nanotubes

In previous studies, we have reported preferential internalization of f-MWNTs by microglia in primary co-culture[20] or following intra-parenchymal injection into the brain tissue[5,6] and have also shown that microglia are involved in the *in vivo* partial degradation of amino-functionalized MWNTs.[14] It was also showed that agglomerates of oxidized MWNTs can be untangled, internalised and then intracellularly processed to some extent by immortalized N9 microglial cells.[15] However,

a

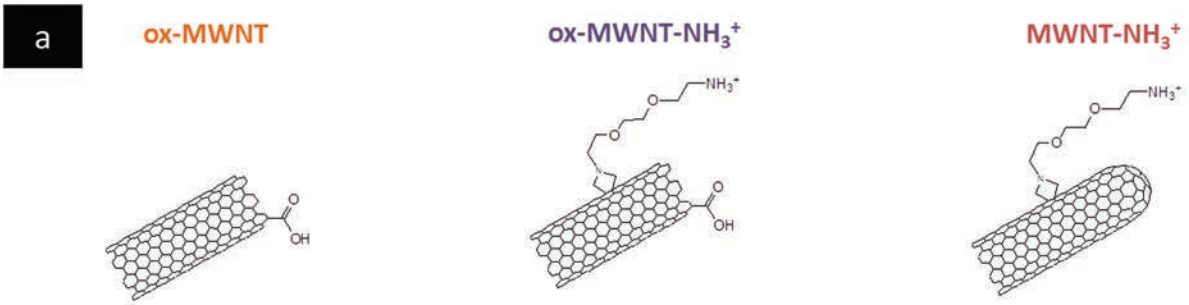

b

Short name	Nature of MWNT	Amount of amino groups (Kaiser test)	Length (TEM)
ox-MWNT	carboxylated	-	200 – 300 nm
ox-MWNT-NH_3^+	carboxylated and aminated (cycloaddition)	170 μmol/g	200 – 300 nm
MWNT-NH_3^+	aminated (cycloaddition)	84 μmol/g	0.5 – 2 μm

c

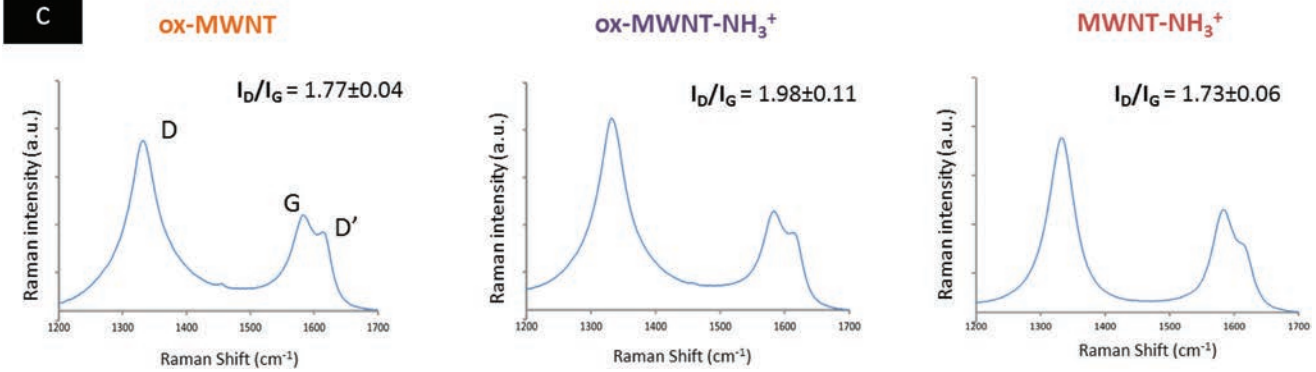

Fig. 1 Characteristics of the different types of functionalized MWNTs. (a) Chemical structures of the different chemically functionalized MWNTs; (b) Table providing the abbreviations used in the manuscript, the length and the amount of amino groups for the different MWNTs; (c) Raman spectra were collected on the starting MWNT suspension before cell exposure. Three characteristic bands are observed: D band at ~1330 cm^{-1}, G band at ~1585 cm^{-1}, and D′ band at ~1620 cm^{-1}. A clearer D′ band was observed for both carboxylated MWNTs, ox-MWNT and ox-MWNT-NH_3^+, in comparison to MWNT-NH_3^+.

the kinetics of degradation and physicochemical characteristics of the MWNTs responsible for the microglia-mediated degradation were not investigated. To address this, and in order to study continuously the biodegradation of carbon nanotubes in the long-term using a relevant *in vitro* model, we developed a specific model of primary microglia cell cultures. We reasoned that to mirror the *in vivo* brain tissue we needed non-dividing cells that can be maintained and monitored for a long period of time (*i.e.* few months) following a single exposure to nanotubes. This would allow monitoring the effects of cells on f-MWNTs measured by Raman spectroscopy at the same particular single cell level and would not be the result of successive cell divisions.

Based on our observations that after one passage, the microglia population was not expanding, we developed microglia-enriched cell cultures with a stable total cell population that could be maintained in 12% FBS completed medium for at least 3 months (with only a normal decrease of the initial population over time, about 30% compared to the initial cell number). In the brain, the define longevity of microglial cells is unknown, but it is widely acknowledged that as specialised tissue macrophages they have a long lifespan – possibly decades in humans – and divide only upon inflammatory activation.[21,22] Here, the enriched microglia cell cultures were obtained after mild trypsination[23] of mixed glial cell cultures isolated from foetal rat brain. Two days after mild trypsination, isolated microglia were exposed for 24 h to 10 μg mL^{-1} of f-MWNT suspensions. This dose was shown previously to be non-toxic for isolated microglia.[20] The next day, f-MWNTs present in the supernatant were removed and the cell monolayers were from

that point maintained in MWNT-free cell culture conditions for various periods of time until Raman analysis.

The timeline of exposure and recovery periods are shown in Fig. 2a. The microscopic aspect of live microglia cells following f-MWNT exposure are also reported for different time points after exposure (Fig. 2b). Optical microscopy images of the exposed cells (live imaging) revealed that microglia internalised a large amount of f-MWNTs irrespective of their surface

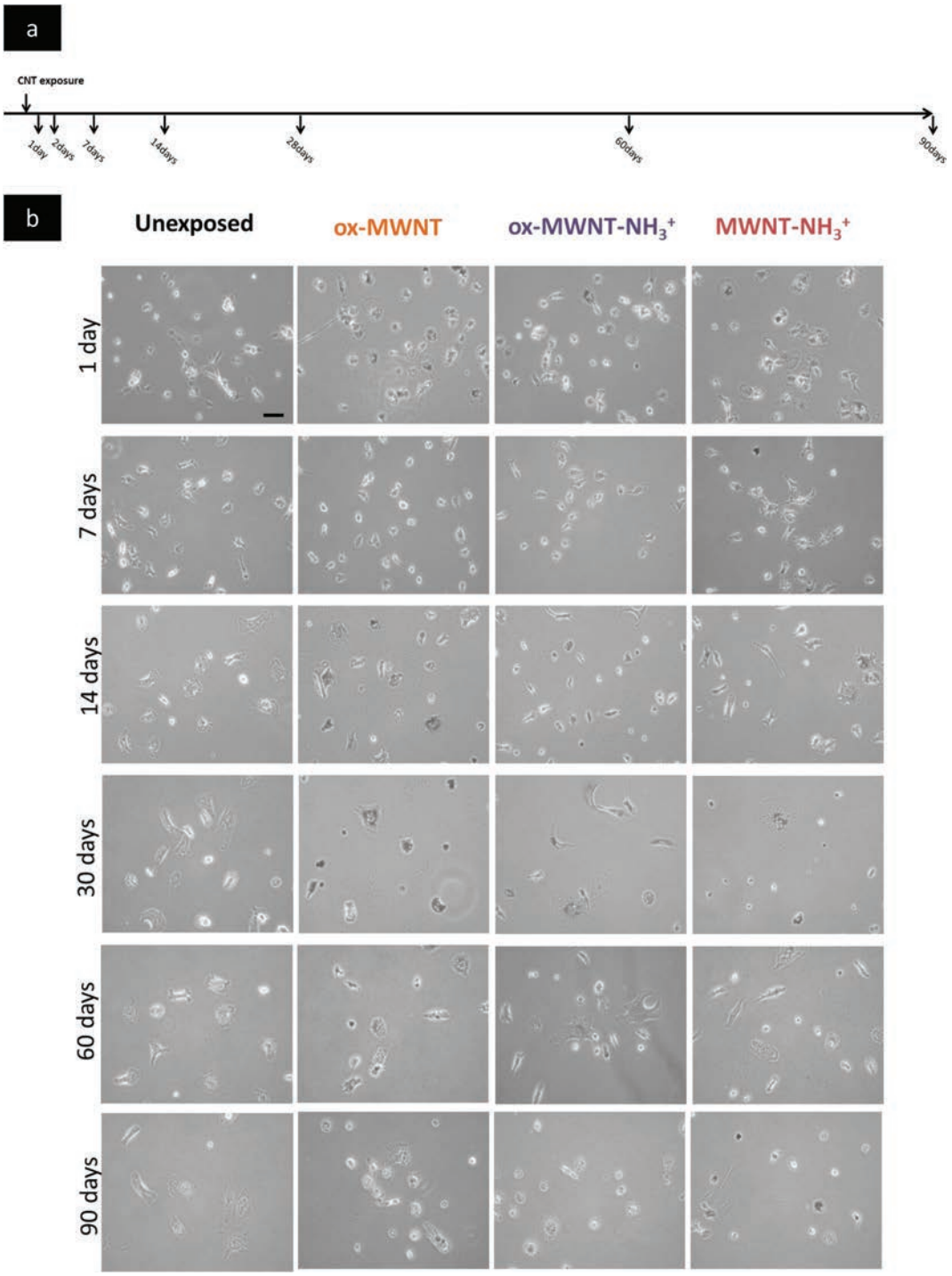

Fig. 2 Live imaging of primary microglia exposed to different functionalized MWNTs *via* optical microscopy. Primary microglia enriched cell cultures were exposed during 24 h to a unique dose of different MWNTs (10 μg mL^{-1}) and then leaved for different period of time before imaging. (a) Schematic of the study design providing the different recovery times after the single exposure to MWNTs. (b) Microglia at day 1 to 90. No significant difference in terms of shape or number of cells was observed between the non-exposed cells and the cells exposed to MWNTs at any time of recovery after the initial exposure. Scale bar = 50 μm.

functionalization. Typically, f-MWNTs appearing as black material accumulated in the perinuclear region probably in phagolysosomes as suggested by the granular aspect of the perinuclear accumulation (for higher magnification see Fig. S1†). The nanotube-loaded vesicles filled almost the whole cytosol, even masking the nucleus when microglial cells were round shaped. Only the nucleus, the extremities and the external boundaries of the cells appeared as clear regions free of f-MWNTs when comparing phase contrast images *versus* bright field images for the same observation field (Fig. S1†). As a function of time, no significant differences were observed in the lightening of the darker regions in cells, or between the different f-MWNTs. This suggested that degradation, if happening, was not complete and did not lead to cells appearing devoid of any material. In addition, there was no difference in terms of shape or number of cells between the different exposures and in comparison to non-exposed cells, indicating that the concentration selected was not affecting cell morphology or viability. Cell morphology is a good indicator of cell response to toxic agents, especially for macrophages and microglia (that act as resident macrophages of the CNS). When macrophages are activated, they usually change their morphology compared to their initial shape. Throughout these experiments, cells exhibited the same normal shape as previously reported.[20,23]

Raman spectroscopy of primary microglia cell culture exposed to functionalized carbon nanotubes

While TEM and XPS analyses of CNTs following intracellular degradation would be greatly helpful to assess respectively the extent of structural alteration[9,24] and the evolution of surface chemistry, they would both require multiple careful steps of extraction and purification in order to avoid introduction of further damages not due to biodegradation and to get access to the CNT surfaces and diameters after their internalisation and intracellular degradative processing. To address the question of the kinetic in the long term, we therefore decided to use a non-destructive and sample preparation-free technique, Raman spectroscopy, which would allow interrogating the structure integrity of CNTs *in situ* without any alteration due to sample processing procedures.

Following the 24 h exposure to different f-MWNTs and a period of recovery from 1 day to 90 days, the microglia cell cultures were washed with PBS (without calcium and magnesium) and then fixed with methanol, in order to minimise the noise on the Raman scattering signal coming from the cell background. Raman spectroscopy was then performed at a single cell level, using the 100× objective of the microscope in order to access the different compartments of a cell (nucleus, cytosol, extremities). Cells were randomly selected over the whole surface of the glass coverslip used as support for the microglia culture. Depending on cell surface, between 12 and 22 spots were selected for Raman spectroscopy analysis within each single cell, as illustrated in Fig. 3. In agreement with the live imaging of microglia (Fig. 2), no difference was observed between the different MWNT exposures or over time in terms of cytoplasmic MWNT loading, while the nucleus appeared clear of any material.

Raman analysis performed in the nuclear region confirmed that no f-MWNTs were accumulated in that region irrespective of the f-MWNTs or the time of recovery considered (data not shown). When Raman spectroscopy was performed in cell regions with the presence of large amounts of dark material, the characteristic peaks of MWNTs (mainly D and G bands, with D′ band on the side of G band) were obtained for all the f-MWNT exposed cells for the duration of the experiment (Table S1†). This suggested that nanotube degradation was not complete, even after 90 days of residency inside microglia, thus confirming our initial optical microscopic observations. These findings are in agreement with many reports showing that MWNTs are carbon nanostructures with a lower degree of degradability compared to SWCNTs or graphene-related materials, mainly attributed to their multi-layered architecture.[9,25] Multi-layered tubes arranged in a concentric manner are likely less degradable than carbon materials consisting of one single layer.

In order to better understand whether the structure of the f-MWNTs have been modified during the period of residency inside the microglia, we calculated the intensity ratio of the D over G bands that is a known indicator of structural modifications and degree of defects. Fig. 4 shows the evolution of the I_D/I_G ratios (and I_D/I_G means) for the different f-MWNTs over time. Structural modifications evidenced by an overall decrease of the mean I_D/I_G ratios from day 1 to 90 were found for all three types of nanotubes (1.95 ± 0.10 to 1.70 ± 0.17 for ox-MWNTs; 2.12 ± 0.10 to 1.87 ± 0.13 for ox-MWNT-NH_3^+; and 1.65 ± 0.15 to 1.49 ± 0.15 for MWNT-NH_3^+). This suggested that a degradative process for all the three types of f-MWNTs was taking place within microglia leading to an accumulation of structural defects. Interestingly, the evolution of I_D/I_G ratios over time was different between the three types of functionalized nanotubes with an initial phase of 15 days during which oxidised nanotubes (ox-MWNTs and ox-MWNT-NH_3^+) exhibited a more rapid pattern of degradation compared to non-oxidised nanotubes (MWNT-NH_3^+), followed by a second phase during which all three nanotubes seemed to undergo further structural deformation but at a similar rate.

For materials bearing free carboxylic functions (ox-MWNTs and ox-MWNT-NH_3^+), evolution of the I_D/I_G ratios between consecutive time points was more significant during the first two weeks after exposure, as evidenced by continuous decrease of the ratio during that period, but was slowing down thereafter with even an increase of the band ratio at 30 and 60 days before decreasing again at 90 days. Materials functionalized with the 1,3-dipolar cycloaddition reaction (MWNT-NH_3^+) also underwent structural modifications from day 1 to 90, but differences in band ratio between consecutive time points were slightly less pronounced than for carboxylated materials during the first two weeks. However, as for oxidized nanotubes, evolution of I_D/I_G ratios at later time points was characterized by alternation of decreasing and increasing levels. These observations suggested that all f-MWNTs degraded over

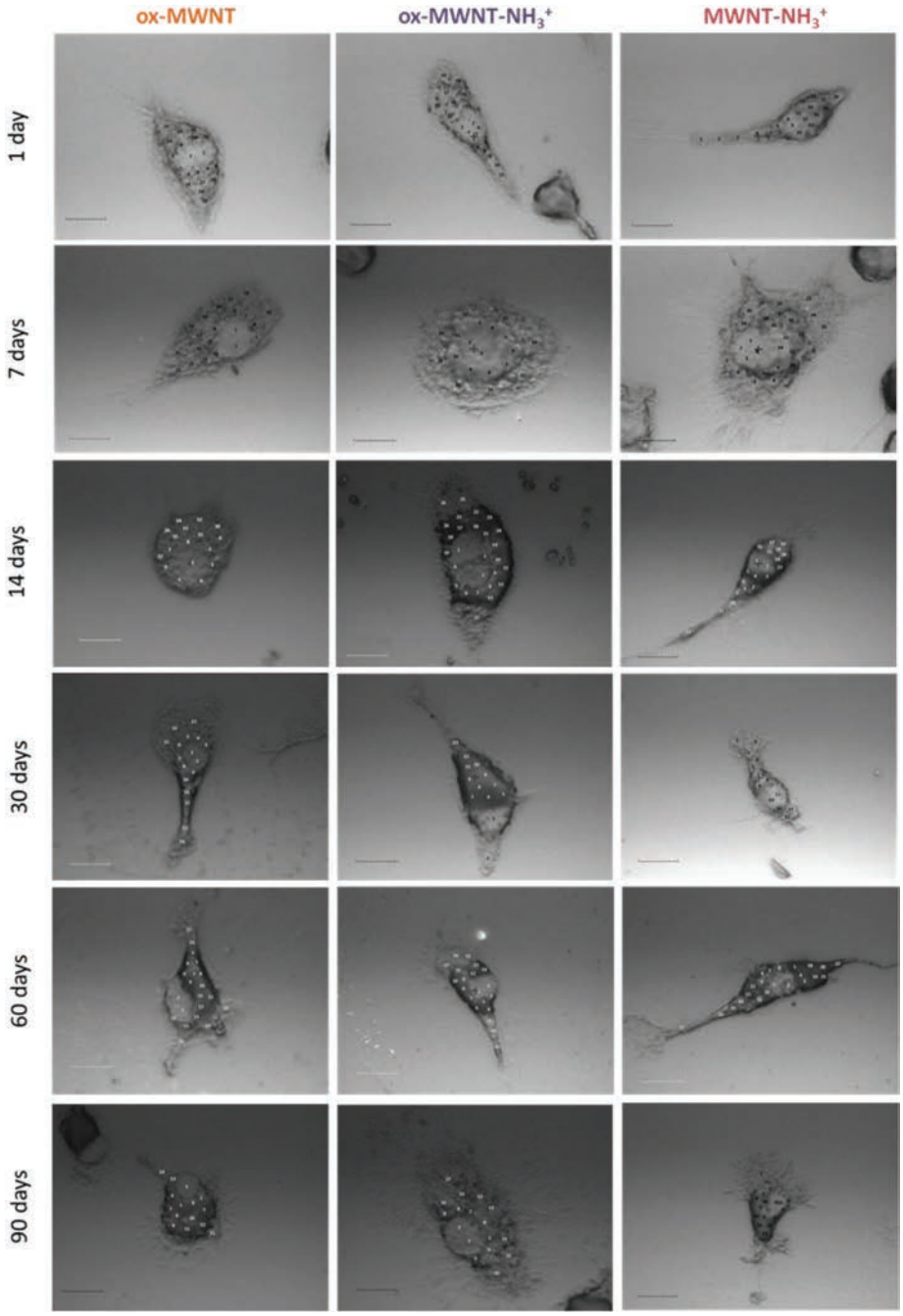

Fig. 3 Optical microscopy of single primary microglial cell before Raman spectroscopy. Primary microglia cultures were fixed with pre-cooled methanol at the end of each desired time and then air dried for at least one hour before further analysis. Representative pictures of single cells observed with a 100× objective in bright field illumination are provided for each exposure and time points, together with numbers showing the typical positions where Raman spectra were collected. No significant difference was observed between the different MWNT exposures. For each cell analysed *via* Raman spectroscopy, three regions could be distinguished: a clear region in the centre of the cell corresponding to the nuclear area where no CNT Raman scattering can be detected, a darker region surrounding the nucleus and attributed to the intracellular accumulation of MWNTs because of the Raman scattering collected, and another clear region delimitating the cell boundaries or extremities where no CNT Raman scattering can be detected. Scale bar = 10 μm.

time in microglia in a non-linear fashion and that the rate and kinetic of degradation of MWNT-NH_3^+ was different from the ones of oxidized nanotubes. The initial presence of higher amount of structural defects on the surface of carboxylated materials, evidenced in Raman spectra by the presence of higher D′ band and due to post-synthesis acidic treatment (Fig. 1), could explain the higher rate of degradation observed for these materials during the first 14 days compared to

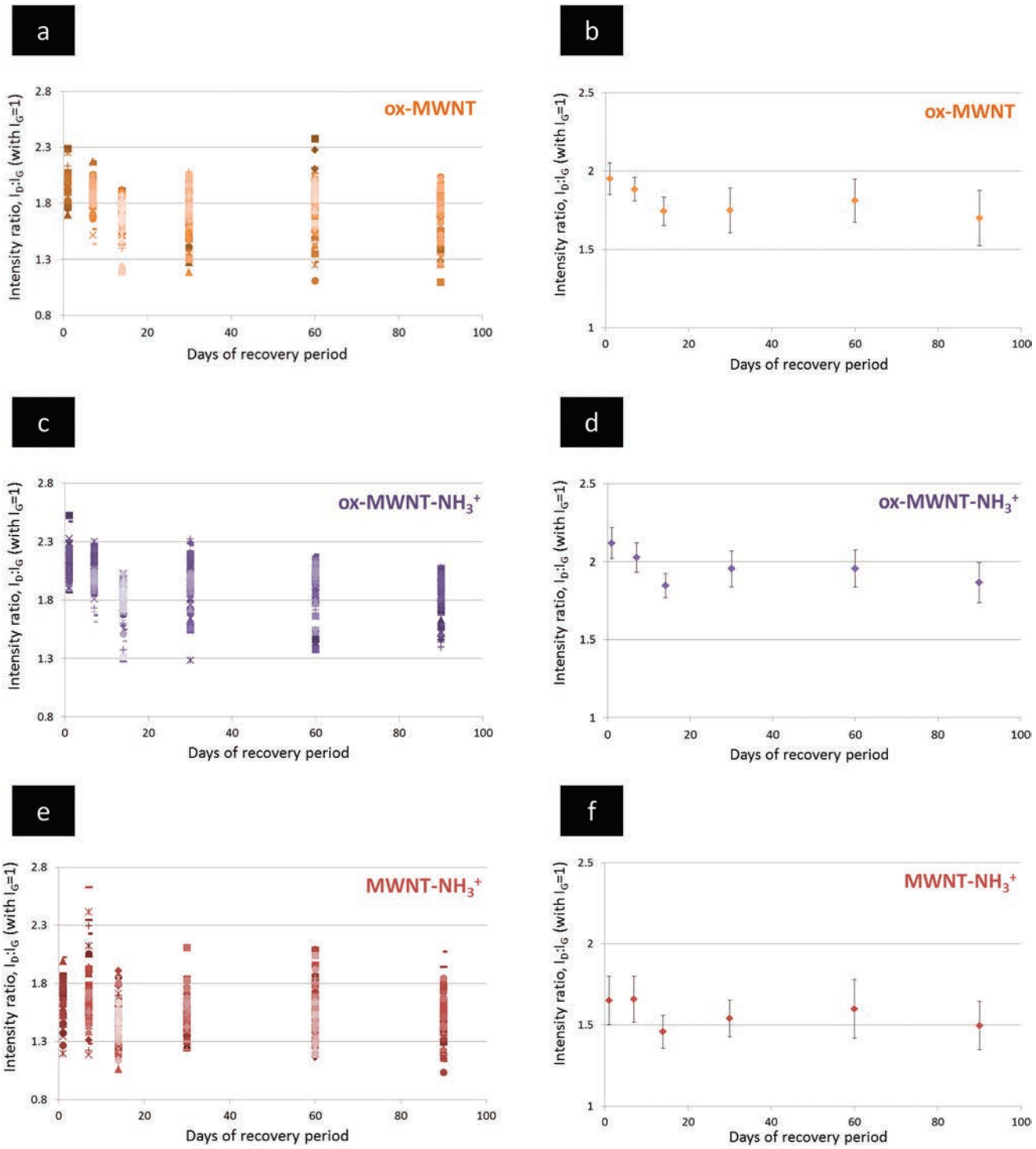

Fig. 4 Raman spectroscopy of microglia cell culture monolayer after exposure to different f-MWNTs. Following the collection of a Raman spectrum, the intensity ratio between D and G bands was calculated from normalised intensity of D and G bands for each spectrum. Intensities were normalised to the intensity of G band (I_G = 1). The intensity I_D/I_G band ratio for all spectra collected (a, c, e) and the average I_D/I_G band ratio (b, d, f) are presented for microglia expose to ox-MWNT (a, b), ox-MWNT-NH_3^+ (c, d) and to MWNT-NH_3^+ (e, f). An overall continuous decrease of I_D/I_G band ratio was observed over time, more significant during the first 14 days for both oxidised materials compared to aminated MWNTs. Between 12 and 22 spectra were collected and analysed for each sample.

non-oxidized nanotubes. Comparisons between oxidized with non-oxidized material (or material with limited amount of oxidation) have shown that a highest degree of degradation is always associated with oxidized nanostructures.[7,10–12,15,26,27] Presumably, the initial structural defects due to oxidation play the role of initiator sites for further structural modifications

(*via* enzyme-catalyzed oxidation processes) leading to higher degradation over time.[10,28] The most defected materials will therefore undergo the highest structural alteration.

A non-linear pattern of structural modifications over time was observed in the present study (sequential increase and decrease of the I_D/I_G band ratio, Fig. 4). This was interpreted as the alternation between two types of previously reported processes. In the first case, evidenced by a decrease of the I_D/I_G band ratio, degradation of CNTs by a defect-consuming process was taking place, whereby defects disappeared with time due to the removal of the damaged parts of the tubes.[29] In the case of functionalized MWNTs, these damaged parts would be primarily the outer walls, not only the functional groups or the outermost layer bearing the functional groups but also the first few outer layers that have been defected due to the functionalization chemical procedures. Therefore, in the present study and amongst the 3 CNTs tested, the fastest to degrade CNTs would be the two types of carboxylated CNTs (ox-MWNTs, ox-MWNT-NH_3^+) that bear significant surface defects due to the oxidation reaction. Layers underneath the oxidized ones would be expected to be more resistant to biodegradation, due to less oxidation defects and a structure close to pristine. This hypothesis is consistent with the results reported here, where a sharp degradation for the two carboxylated CNTs was observed over the first two weeks (*i.e.* degradation of the few outermost defected layers), followed by a much slower degradation pattern over time (*i.e.* of the remaining deeper layers that are significantly less defected). In the second type of degradation processes previously reported, more defects appeared on the surface (in addition to the pre-existing ones) due to enzyme-catalyzed oxidation leading to an increase of the ratio, mainly attributed to higher D band intensity.[25,30,31] In agreement with the latter statement, when Raman spectroscopy was performed on microglia exposed to MWNT-NH_3^+ at 30, 60 and 90 days, we observed in some cases the appearance of a clear D′ band in correlation with an increase of the D peak intensity also known as indication of higher structural defects, as shown in Fig. 5. Considering that the starting MWNT-NH_3^+ materials did not display a clear D′ band (Fig. 1), this suggested that MWNT-NH_3^+ were undergoing degradation *via* a defect-accumulating process, possibly oxidation *via* reactive oxygen species as reported previously.[9] In order to prove or dispute any of these working hypotheses of degradation mechanisms, specific further experiments will be required. For instance, studies addressing the evolution of CNT diameters over time using TEM would help to reveal the real mechanisms at stake and to compare to previous studies.[7,24,32] But this was not in the scope of the present study focusing on the kinetic of degradation in the long term.

Although carbon nanostructures have been assumed resilient due to their strong inert sp^2 hybridised carbon structure, their degradation under physiological conditions is now well acknowledged.[8,28,33] Since the first demonstration that SWCNTs,[12,34] MWNTs[10] and graphene[27,35] can all undergo oxidation-based degradation after incubation with peroxidases in the presence of H_2O_2, there have been numerous reports of

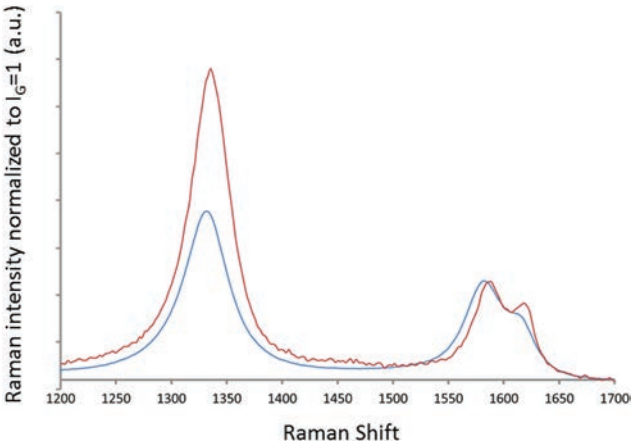

Fig. 5 Raman spectroscopy of MWNT-NH_3^+. For some Raman spectra collected in primary microglia exposed to MWNT-NH_3^+ at late time points (30, 60, 90 days), we observed a distinct D′ band next to the G band (red spectrum), in contrast to the starting MWNT-NH_3^+ material (blue spectrum) in which this D′ band was absent. A representative spectrum of this phenomenon is provided for MWNT-NH_3^+ exposed microglia analysed at 90 day time point.

such oxidation-mediated processes taking place both *in vitro* and *in vivo*. Immune cells involved in the pulmonary response to CNTs such as neutrophils and eosinophils were successively reported to be able to digest SWNTs, by the action of myeloperoxidase and eosinophil peroxidase respectively.[32,36] It was then shown at the *in vivo* level that degradation of SWNTs *via* the myeloperoxidase-mediated oxidation process was occurring in the lungs of animals after pharyngeal aspiration.[37] In addition, carboxyl functionalized graphene was also shown to degrade over a period of 3 months in the resident macrophages of various tissues such as lung, liver, kidney and spleen.[38] After 3 months, the highest degree of degradation leading to amorphous carbon was documented in the spleen which is one of the major organs of the mononuclear phagocytic system.[39] With regards to brain, we have previously reported that microglia were the main cells responsible for the *in situ* internalisation and degradation of f-MWNTs injected directly in the cortical parenchyma.[14] In agreement with the results reported here, we observed an overall decrease of the I_D/I_G ratio over a period of 14 days for MWNT-NH_3^+ albeit to a different extent as *in vivo* degradation seemed to be a more dynamic process involving more cells (such as brain perivascular macrophages) and potentially clearance mechanisms than a static *in vitro* model of isolated microglia. While the exact biodegradation mechanism and kinetics remain here elusive and will require more in-depth *in vitro* investigations, we can foresee that *in vivo* studies will be required to fully understand the extent of degradability of carbon nanomaterials in the long term.

Biodegradation of carbon nanomaterials is seen as a way to eliminate carbon-based vector and therapeutic or diagnostic transport systems after achieving their function.[33] However, biodegradative processes should also be considered as potential determinants of the overall toxicological profile of nano-

materials due to the uncertain nature and impact of the degradation by-products.[40] Not only degradation can potentially lead to production of by-products of more acute cytotoxicity than the starting non-degraded material, but also can form transient nanostructures some of which may have shown higher toxicity. For example, one of the possible issues resulting from degradation of thicker MWNTs is the production of thinner MWNTs due to peeling/exfoliation of outer layers. Thinner MWNTs have been shown to pose a higher toxicological risk than thicker nanotubes.[41,42] Reassuringly, two studies have shown that CNTs that degraded in test tube under specific conditions and then administrated in animals did not induce any toxic effects. In the first study, biodegraded SWNTs administered by pharyngeal aspiration did not induce inflammatory responses.[32] In the second study, MWNTs shortened by a 10 week long treatment in phagolysosome-mimicking solution did not produce any pathogenic effects after injection in the peritoneal cavity.[43] Amino functionalized MWNTs (*via* arylation) processed for 24 h in THP-1 derived macrophages were also assessed for their cytotoxicity after extraction.[9] THP-1 processed MWNTs displaying holes in their walls were shown to be less toxic to THP-1 cells than the original (non-predigested) nanotubes. Similarly, in a previous study[20] or in the present study (Fig. 2a and b) we did not observe any toxic or obvious deleterious effects on the microglial cells at the concentration used here (*i.e.* 10 μg mL^{-1}) even after 90 days. Since occurrence of degradation is confirmed over time, further experiments focusing on the microglial cell functionality at this non-toxic concentration will answer definitely to the question of possible damaging effects of the by-products.

Among all the studies of carbon nanostructure degradation that have been reported in the literature, surface properties have emerged as a determinant parameter of the rate of degradation. Degree of carboxylation was shown to directly impact on the ability of materials to degrade. Graphene oxide was shown to degrade after incubation with HRP and myeloperoxidase, whereas a reduced form of graphene oxide was unable to undergo degradation under similar conditions.[27,35] Li *et al.* confirmed those findings and also found that graphene oxide non-covalently functionalized with bovine serum albumin or PEG was resistant to HRP mediated oxidation.[11] They also suggested that the protein coating prevented the close interaction between the graphene oxide with the peroxidase, therefore limiting its further oxidation and degradation. In contrast, covalently PEGylated SWNTs were shown to degrade in various peroxidase containing solutions.[44] Interestingly, when graphene oxide was covalently PEGylated *via* a cleavable bond, when incubated under conditions that favoured bond cleavage, the released graphene oxide could undergo degradation in a similar manner as bare graphene oxide.[11] In another study, the amount of defects in the graphitic lattice of the carbon nanomaterials was also shown to be an important parameter, as evidence by a quicker degradation of nitrogen-doped MWNTs compared to oxidised MWNTs.[10] Such findings also demonstrate that degradability of carbon nanomaterials can be tailored by surface functionalization as some of us recently illustrated,[13] opening up the possibility to exciting future investigations of engineering degradability cues and effectors on the surface of the nanomaterial.

Conclusions

The present study reports the evolution over time of the Raman signature of different functionalized carbon nanotubes internalized inside primary microglia. The accumulating structural changes of intracellularly-localized carbon nanotubes were attributed to partial degradation of the materials inside cells that varied according to their initial type of surface functionalization. While surface carboxylation enhanced degradation during the first two weeks in comparison to amination, no difference in the rate and kinetics of degradation was then observed between carboxylation and amination. Irrespective of the type of chemical functionalization, partial degradation occurred for all types of nanotubes and was progressive over the timeline of the study (90 days). Overall it can be described as a slow but continuous process. These findings highlight the importance of surface chemical functionalization toward the development of carbon nanomaterials not only biocompatible but also with tailored biodegradability,[13,33] in particular for biomedical applications in the CNS.

Experimental

Materials

Multiwalled carbon nanotubes (MWNT) were purchased from Nanostructured and Amorphous Materials Inc. (Houston, TX, USA; Lot # 1240XH, 95%). The outer average diameter was 20–30 nm, and the length was 0.5–2 μm. The chemicals and solvents were obtained from Sigma-Aldrich (UK). Cell culture reagents (PBS, trypsin, foetal bovine serum, DMEM : F12) were purchased from Gibco (Life technologies, UK). The different chemical functionalizations of multi-walled carbon nanotubes were performed following well-established procedures previously reported by our groups.[16–18,45,46] The amount of COOH after the oxidation reaction as been previously calculated using thermogravimetric analysis, corresponding to 1,7 μmol g^{-1}.[25]

Preparation of MWNTs for cell exposure

A 1 mg mL^{-1} stock suspension of functionalized MWNTs was prepared with sterile 5% dextrose in distilled water, sonicated 45 min and stored at −20 °C before further use. After thawing, the CNT suspension was sonicated 10 min before further dilution (10 μg mL^{-1}) in serum free cell culture medium. Sterile dextrose solution was used as control with cells non-exposed to CNTs; a 0.05% dextrose solution (500 μg mL^{-1}) was prepared with serum free cell culture medium.

Primary cell cultures

Primary mixed glial cell cultures. Mixed glial cell cultures were prepared with striatum extracted from E16–E18 Wistar

foetal rat brains (standard Witschi stages 33–34). Striatal tissue pieces were dissociated to single cell suspensions by trypsinisation followed by mechanical trituration in Ca^{2+}/Mg^{2+} free HBSS solution.[47,48] After determination of the number of live cells, six millions of cells were plated onto poly-D-lysine (50 μg ml^{-1}) coated 75 cm^2 flask with DMEM : F12 medium completed with 12% heat inactivated foetal bovine serum and incubated at 37 °C in a humidified 5% CO_2 incubator. Medium was changed daily for a 10 days period, after which the cell monolayer was trypsinised, splitted (2/3 ratio), and seeded onto 60 mm glass coverslips coated with poly-L-lysine (50 μg ml^{-1}) that were individually hosted in 6 well plates.

Primary microglia enriched cell cultures. Microglia enriched cell cultures were prepared from striatal mixed glial cultures at passage 1, according to previously described method, based on mild trypsinisation.[23] At confluence, the cell monolayer on glass coverslip was treated with trypsin diluted in serum free DMEM : F12 medium (final trypsin concentration 0.05%) until all cells detached, except microglial cells which remained attached to the glass coverslip. After washing with serum free DMEM : F12 medium, cells were cultured in DMEM : F12 medium completed with 12% heat inactivated foetal bovine serum. Cells obtained after this treatment were all positive for CD11b/c (clone OX42) (data not shown). After 48 h incubation, microglia enriched cell cultures were treated with CNTs (10 μg mL^{-1}).

Exposure of microglial cells to functionalized MWNTs

Microglia enriched cell cultures were first exposed for 2 h to a 10 μg mL^{-1} CNT suspension prepared in serum free cell culture medium (DMEM : F12 medium). After 2 h incubation at 37 °C without serum, the cell culture medium was completed with heat inactivated foetal bovine serum (12%). After 24 h incubation at 37 °C, the supernatant – still containing CNTs – was removed, cells were washed twice with PBS and then incubated with CNT free complete medium (DMEM : F12 with 12% serum) for 1, 7, 14, 30, 60 and 90 days (recovery period). CNT free complete medium was changed every 3 days. At the end of exposure, cells on glass coverslips were washed twice with PBS and then fixed with methanol, previously cooled at −20 °C, for 10 min at −20 °C. The glass coverslips were then removed from the well plates, air dried for at least 1 hour under the air flow of a microbiology safety cabinet, fixed on microscopy glass slide with nail polish, and stored in slide boxes at room temperature until further Raman analysis.

Raman spectroscopy

Raman spectroscopic analyses were performed with a Thermo Scientific DXR Raman microscope, equipped with an Olympus microscope and a 633 nm LASER, using a 100× objective lens and 1 mW of LASER power. Each spectrum has been recorded on a specific spot area (1 μm^2) randomly selected within the cell demarcations (see Fig. 3 as example of spot map). Each spectrum recorded is the average of 3 times 50 s of LASER illumination for one spot. For each cell randomly selected within the cells covering the glass coverslip, between 12 and 22 spectra were recorded, depending on the cell surface. A minimum of 10 cells per samples (3 different CNTs and 6 different time points) have been analysed by Raman microscopy. Each spectrum were analysed individually to determine the highest intensity of the different characteristic peaks for CNTs, meaning G, D, D′ and G′ (2D) bands.[49–51] Raman spectra were corrected for cell autofluorescence (fluorescence coming from the cell and the glass support) and normalised to G band intensity (I_G = 1) so as to determine the I_D/I_G band ratio.

Acknowledgements

This work was supported by the European Commission, under the FP-7 *Marie Curie* actions, (Career Development Intra-European Fellowship, PIEF-GA-2010-276051, project NANONEUROHOP). AB wishes to thank the CNRS financial support from PICS (Project for International Scientific Cooperation). The authors also thank T. Bernard for her help during the analysis of the Raman data.

References

1 A. Battigelli, C. Menard-Moyon, T. Da Ros, M. Prato and A. Bianco, *Adv. Drug Delivery Rev.*, 2013, **65**, 1899–1920.
2 B. S. Wong, S. L. Yoong, A. Jagusiak, T. Panczyk, H. K. Ho, W. H. Ang and G. Pastorin, *Adv. Drug Delivery Rev.*, 2013, **65**, 1964–2015.
3 A. Nunes, K. Al-Jamal, T. Nakajima, M. Hariz and K. Kostarelos, *Arch. Toxicol.*, 2012, **86**, 1009–1020.
4 H. J. Lee, J. Park, O. J. Yoon, H. W. Kim, Y. Lee do, H. Kim do, W. B. Lee, N. E. Lee, J. V. Bonventre and S. S. Kim, *Nat. Nanotechnol.*, 2011, **6**, 121–125.
5 K. T. Al-Jamal, L. Gherardini, G. Bardi, A. Nunes, C. Guo, C. Bussy, M. A. Herrero, A. Bianco, M. Prato, K. Kostarelos and T. Pizzorusso, *Proc. Natl. Acad. Sci. U. S. A.*, 2011, **108**, 10952–10957.
6 G. Bardi, A. Nunes, L. Gherardini, K. Bates, K. T. Al-Jamal, C. Gaillard, M. Prato, A. Bianco, T. Pizzorusso and K. Kostarelos, *PLoS One*, 2013, **8**, e80964.
7 G. P. Kotchey, S. A. Hasan, A. A. Kapralov, S. H. Ha, K. Kim, A. A. Shvedova, V. E. Kagan and A. Star, *Acc. Chem. Res.*, 2012, **45**, 1770–1781.
8 K. Bhattacharya, F. T. Andon, R. El-Sayed and B. Fadeel, *Adv. Drug Delivery Rev.*, 2013, **65**, 2087–2097.
9 D. Elgrabli, W. Dachraoui, C. Menard-Moyon, X. J. Liu, D. Begin, S. Begin-Colin, A. Bianco, F. Gazeau and D. Alloyeau, *ACS Nano*, 2015, **9**, 10113–10124.
10 Y. Zhao, B. L. Allen and A. Star, *J. Phys. Chem. A*, 2011, **115**, 9536–9544.
11 Y. Li, L. Feng, X. Shi, X. Wang, Y. Yang, K. Yang, T. Liu, G. Yang and Z. Liu, *Small*, 2014, **10**, 1544–1554.
12 B. L. Allen, G. P. Kotchey, Y. Chen, N. V. Yanamala, J. Klein-Seetharaman, V. E. Kagan and A. Star, *J. Am. Chem. Soc.*, 2009, **131**, 17194–17205.

13 A. R. Sureshbabu, R. Kurapati, J. Russier, C. Menard-Moyon, I. Bartolini, M. Meneghetti, K. Kostarelos and A. Bianco, *Biomaterials*, 2015, **72**, 20–28.
14 A. Nunes, C. Bussy, L. Gherardini, M. Meneghetti, M. A. Herrero, A. Bianco, M. Prato, T. Pizzorusso, K. T. Al-Jamal and K. Kostarelos, *Nanomedicine*, 2012, **7**, 1485–1494.
15 A. E. Goode, D. A. Gonzalez Carter, M. Motskin, I. S. Pienaar, S. Chen, S. Hu, P. Ruenraroengsak, M. P. Ryan, M. S. Shaffer, D. T. Dexter and A. E. Porter, *Biomaterials*, 2015, **70**, 57–70.
16 S. P. Li, W. Wu, S. Campidelli, V. Sarnatskaia, M. Prato, A. Tridon, A. Nikolaev, V. Nikolaev, A. Bianco and E. Snezhkova, *Carbon*, 2008, **46**, 1091–1095.
17 V. Georgakilas, K. Kordatos, M. Prato, D. M. Guldi, M. Holzinger and A. Hirsch, *J. Am. Chem. Soc.*, 2002, **124**, 760–761.
18 V. Georgakilas, N. Tagmatarchis, D. Pantarotto, A. Bianco, J. P. Briand and M. Prato, *Chem. Commun.*, 2002, 3050–3051.
19 M. S. Dresselhaus, G. Dresselhaus, A. Jorio, A. G. Souza and R. Saito, *Carbon*, 2002, **40**, 2043–2061.
20 C. Bussy, K. T. Al-Jamal, J. Boczkowski, S. Lanone, M. Prato, A. Bianco and K. Kostarelos, *ACS Nano*, 2015, **9**, 7815–7830.
21 K. Saijo and C. K. Glass, *Nat. Rev. Immunol.*, 2011, **11**, 775–787.
22 M. Prinz and J. Priller, *Nat. Rev. Neurosci.*, 2014, **15**, 300–312.
23 J. Saura, J. M. Tusell and J. Serratosa, *Glia*, 2003, **44**, 183–189.
24 V. E. Kagan, A. A. Kapralov, C. M. St Croix, S. C. Watkins, E. R. Kisin, G. P. Kotchey, K. Balasubramanian, I. I. Vlasova, J. Yu, K. Kim, W. Seo, R. K. MallampaIli, A. Star and A. A. Shvedova, *ACS Nano*, 2014, **8**, 5610–5621.
25 J. Russier, C. Menard-Moyon, E. Venturelli, E. Gravel, G. Marcolongo, M. Meneghetti, E. Doris and A. Bianco, *Nanoscale*, 2011, **3**, 893–896.
26 X. Liu, R. H. Hurt and A. B. Kane, *Carbon*, 2010, **48**, 1961–1969.
27 G. P. Kotchey, B. L. Allen, H. Vedala, N. Yanamala, A. A. Kapralov, Y. Y. Tyurina, J. Klein-Seetharaman, V. E. Kagan and A. Star, *ACS Nano*, 2011, **5**, 2098–2108.
28 G. P. Kotchey, Y. Zhao, V. E. Kagan and A. Star, *Adv. Drug Delivery Rev.*, 2013, **65**, 1921–1932.
29 C. F. Chiu, B. A. Barth, G. P. Kotchey, Y. Zhao, K. A. Gogick, W. A. Saidi, S. Petoud and A. Star, *J. Am. Chem. Soc.*, 2013, **135**, 13356–13364.
30 V. Neves, E. Heister, S. Costa, C. Tilmaciu, E. Borowiak-Palen, C. E. Giusca, E. Flahaut, B. Soula, H. M. Coley, J. McFadden and S. R. P. Silva, *Adv. Funct. Mater.*, 2010, **20**, 3272–3279.
31 Y. Sato, A. Yokoyama, Y. Nodasaka, T. Kohgo, K. Motomiya, H. Matsumoto, E. Nakazawa, T. Numata, M. Zhang, M. Yudasaka, H. Hara, R. Araki, O. Tsukamoto, H. Saito, T. Kamino, F. Watari and K. Tohji, *Sci. Rep.*, 2013, **3**, 2516.
32 V. E. Kagan, N. V. Konduru, W. Feng, B. L. Allen, J. Conroy, Y. Volkov, I. I. Vlasova, N. A. Belikova, N. Yanamala, A. Kapralov, Y. Y. Tyurina, J. Shi, E. R. Kisin, A. R. Murray, J. Franks, D. Stolz, P. Gou, J. Klein-Seetharaman, B. Fadeel, A. Star and A. A. Shvedova, *Nat. Nanotechnol.*, 2010, **5**, 354–359.
33 A. Bianco, K. Kostarelos and M. Prato, *Chem. Commun.*, 2011, **47**, 10182–10188.
34 B. L. Allen, P. D. Kichambare, P. Gou, I. I. Vlasova, A. A. Kapralov, N. Konduru, V. E. Kagan and A. Star, *Nano Lett.*, 2008, **8**, 3899–3903.
35 R. Kurapati, J. Russier, M. A. Squillaci, E. Treossi, C. Menard-Moyon, A. E. Del Rio-Castillo, E. Vazquez, P. Samori, V. Palermo and A. Bianco, *Small*, 2015, **11**, 3985–3994.
36 F. T. Andon, A. A. Kapralov, N. Yanamala, W. Feng, A. Baygan, B. J. Chambers, K. Hultenby, F. Ye, M. S. Toprak, B. D. Brandner, A. Fornara, J. Klein-Seetharaman, G. P. Kotchey, A. Star, A. A. Shvedova, B. Fadeel and V. E. Kagan, *Small*, 2013, **9**, 2721–2729.
37 A. A. Shvedova, A. A. Kapralov, W. H. Feng, E. R. Kisin, A. R. Murray, R. R. Mercer, C. M. St Croix, M. A. Lang, S. C. Watkins, N. V. Konduru, B. L. Allen, J. Conroy, G. P. Kotchey, B. M. Mohamed, A. D. Meade, Y. Volkov, A. Star, B. Fadeel and V. E. Kagan, *PLoS One*, 2012, **7**, e30923.
38 C. M. Girish, A. Sasidharan, G. S. Gowd, S. Nair and M. Koyakutty, *Adv. Healthcare Mater.*, 2013, **2**, 1489–1500.
39 L. C. Davies, S. J. Jenkins, J. E. Allen and P. R. Taylor, *Nat. Immunol.*, 2013, **14**, 986–995.
40 S. Lanone, P. Andujar, A. Kermanizadeh and J. Boczkowski, *Adv. Drug Delivery Rev.*, 2013, **65**, 2063–2069.
41 H. Nagai, Y. Okazaki, S. H. Chew, N. Misawa, Y. Yamashita, S. Akatsuka, T. Ishihara, K. Yamashita, Y. Yoshikawa, H. Yasui, L. Jiang, H. Ohara, T. Takahashi, G. Ichihara, K. Kostarelos, Y. Miyata, H. Shinohara and S. Toyokuni, *Proc. Natl. Acad. Sci. U. S. A.*, 2011, **108**, E1330–E1338.
42 I. Fenoglio, E. Aldieri, E. Gazzano, F. Cesano, M. Colonna, D. Scarano, G. Mazzucco, A. Attanasio, Y. Yakoub, D. Lison and B. Fubini, *Chem. Res. Toxicol.*, 2012, **25**, 74–82.
43 M. J. Osmond-McLeod, C. A. Poland, F. Murphy, L. Waddington, H. Morris, S. C. Hawkins, S. Clark, R. Aitken, M. J. McCall and K. Donaldson, *Part. Fibre Toxicol.*, 2011, **8**, 15.
44 I. I. Vlasova, T. V. Vakhrusheva, A. V. Sokolov, V. A. Kostevich, A. A. Gusev, S. A. Gusev, V. I. Melnikova and A. S. Lobach, *Toxicol. Appl. Pharmacol.*, 2012, **264**, 131–142.
45 H. Ali-Boucetta, K. T. Al-Jamal, K. H. Muller, S. Li, A. E. Porter, A. Eddaoudi, M. Prato, A. Bianco and K. Kostarelos, *Small*, 2011, **7**, 3230–3238.
46 K. T. Al-Jamal, H. Nerl, K. H. Muller, H. Ali-Boucetta, S. Li, P. D. Haynes, J. R. Jinschek, M. Prato, A. Bianco, K. Kostarelos and A. E. Porter, *Nanoscale*, 2011, **3**, 2627–2635.
47 T. Fath, Y. D. Ke, P. Gunning, J. Gotz and L. M. Ittner, *Nat. Protoc.*, 2009, **4**, 78–85.

48 M. Ni and M. Aschner, *Current Protocols Toxicology*, 2010, ch. 12, Unit 12 17.
49 M. S. Dresselhaus, G. Dresselhaus, R. Saito and A. Jorio, *Phys. Rep.*, 2005, **409**, 47–99.
50 M. S. Dresselhaus, A. Jorio, M. Hofmann, G. Dresselhaus and R. Saito, *Nano Lett.*, 2010, **10**, 751–758.
51 A. Cuesta, P. Dhamelincourt, J. Laureyns, A. Martinezalonso and J. M. D. Tascon, *Carbon*, 1994, **32**, 1523–1532.